CL-Windcon

Closed Loop Wind Farm Control

DELIVERABLE REPORT

Optimized farm layout

Deliverable No.	D4.3	Work Package No.	WP4	Tasks No.	4.3.1
Work Package Title		Feasibility			
Linked Tasks Title		Wind Farm Framework Redesign			
Status		**Final**			
Dissemination level		**public**			
Due date deliverable		2019-06-30		Submission date	2019-06-29
Deliverable version		D4.3 Optimized Farm Layout - Final			

This project has received funding from the European Union's Horizon 2020 research and innovation programme under grant agreement No 727477

DOCUMENT CONTRIBUTORS

Deliverable responsible	USTUTT
Contributor	**Organization**
Mohammad Salari	USTUTT
Torben Knudsen	AAU
Giancarlo Potenza	EGP

Reviewer	**Organization**
Filippo Campagnolo	TUM
Juan Cristóbal García	Zabala

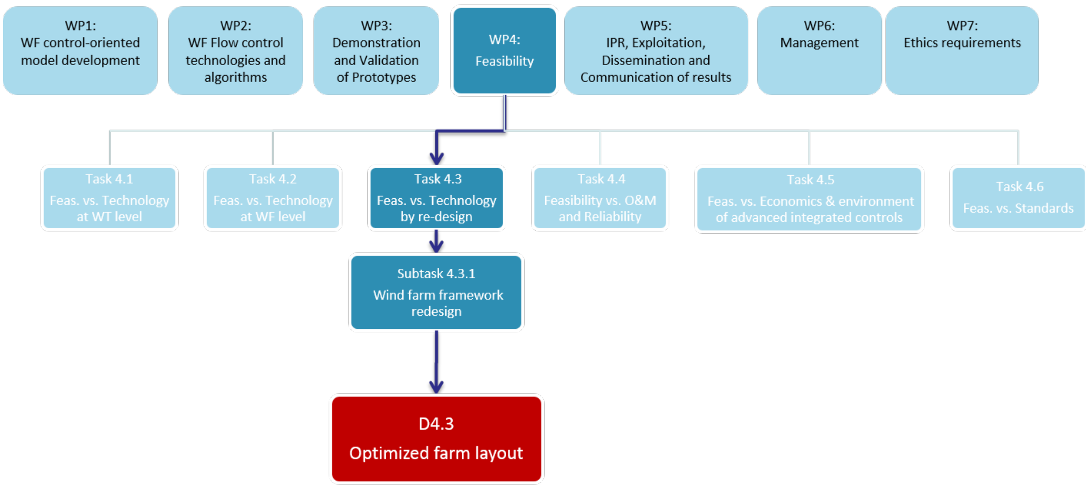

Map of work-package 4 and its subtasks and position of Deliverable D4.3

CONTENTS

LIST OF FIGURES

LIST OF TABLES

1 EXECUTIVE SUMMARY

For designing a wind farm the two most important KPIs that should be considered are the wind farm power and the fatigue loads. The wind farm layout can play a key role to increase the annual energy production (AEP) of wind farm and to decrease the fatigue loads on the wind turbines. In addition to wind farm layout, the optimization of yaw setting can also be used for the sake of above KPIs. Another important KPI to be considered when a wind farm is in design stage is the distance between the turbines. The costs can increase when the distance between turbines increase. This can be because of e.g. cabling, operation and maintenance, and installations cost which increase with wind farm size.

This deliverable first deals with layout optimization, yaw optimization and a combined layout/yaw optimization of NORCOWE RWF in Deliverable D1.1 [3]: *Definition of reference wind farms and simulation scenarios*. The objective function for the optimization is to maximize the AEP of the wind farm. WISDEM [28] and OpenMDAO [18] are the tools which are used for the optimization. The used wake model is the parametric wind turbine wake model FLORIS (FLOw Redirection and Induction in Steady-state). It has been shown that position optimization has bigger contribution in increasing AEP than yaw optimization. Also because of (probably) numerical error in OpenMDAO a combined layout/yaw optimization has been carried out for fewer number of wind turbines (maximum 70 turbines). The used wind data are from FINO3 [8] met mast for years 2000-2010 from which two different wind roses with 6 and 12 bins are made. These wind roses together with turbine data are the input to the optimization problem. The constraints for the optimization problem are the rectangular bound around the wind farm as well as the minimum distances between the turbines. The best optimization result is achieved by combined layout/yaw optimization with an improvement of 34.02%.

This deliverable then studies the redesign of wind farm using induction control. Without farm control if the wind farm is squeezed in size, energy production will decrease and loads will increase. The potential of using induction control only method is investigated to see how much of these losses can be compensated. The controller will be the FF controller described in Deliverable D4.2 [4]: *Hardware and infrastructure conditions for energy capture and fatigue improvements* section 5.1 which is based on a analytic optimization using the static Jensen model. SimWindFarm will be used for simulation and the farm considered is the 3x3 CL-Windcon wind farm from Deliverable D1.1 [3]. It has been seen that the optimal feed forward control improves the power performance between 0.5 and 1%. This leads to a squeezing of the farm length scale by 3% without loosing power performance and with improved fatigue performance for main shaft and tower.

2 WIND FARM LAYOUT AND YAW SETTING OPTIMIZATION

2.1 Introduction

Due to increasing energy consumption and the goal of reaching an energy supply mainly covered by renewable energies, it is necessary to improve existing energy production concepts and make them more efficient. In the area of wind energy production, the size of wind turbines has grown steadily in the past and there have been rapid developments in wind turbine technology. For example, the average installed Power per wind turbine in Germany has grown from 2.76 MW in 2014 to 3.30 MW in 2017 [26]. Wind turbines are often grouped in the same location - both onshore and offshore - to increase the maximum usable power out of the wind and to use synergy effects. The optimal layout of a wind farm depends on many site-specific parameters like meteorological conditions, limitation of available area, grid connection, cabling, regulations, etc. By planning the layout, it has to be taken into account that the positioning of the turbines within the wind farm has great impact on the power production and therefore on the cost of energy.

The main goal of planning a wind farm layout is to maximize the energy production with minimal fatigue and minimal space between the turbines. In a wind farm the layout is of the high importance to the annual energy production (AEP) as the wake of a turbine is influencing the power production of other turbines standing in its path.To maximize the AEP, and to decrease the fatigue loads on the turbines, the turbines have to be placed in such way that the wake effects between turbines are minimized.

In addition to wind farm layout, the controller of a wind farm can be used to increase the power production and to decrease the loads by deflecting the wake of a turbine away from downstream turbines [10]. When a wind turbine works in yaw, the efficiency of this turbine is reduced in order to increase the power production of downstream turbines [24]. The wake deflection due to a turbine in wake is shown in Figure 1.

The correct understanding of how the wake propagates within the wind farm and how the velocity is distributed in the wake is essential. There are different wake models available which can be divided into two groups: Analytical and computational wake models [22]. It cannot be expected that the models are able to characterize the wake in detail, but when used properly, they are sufficient in means of estimating the power production of a wind farm. Nevertheless, it needs to be kept in mind that in a worst-case scenario, smallest deviations in the prediction of the wake can lead to a lower AEP of the wind farm. The search for the optimal wind farm layout under consideration of a wake model is a multidisciplinary optimization problem, which has to be solved by using numerical simulation tools.

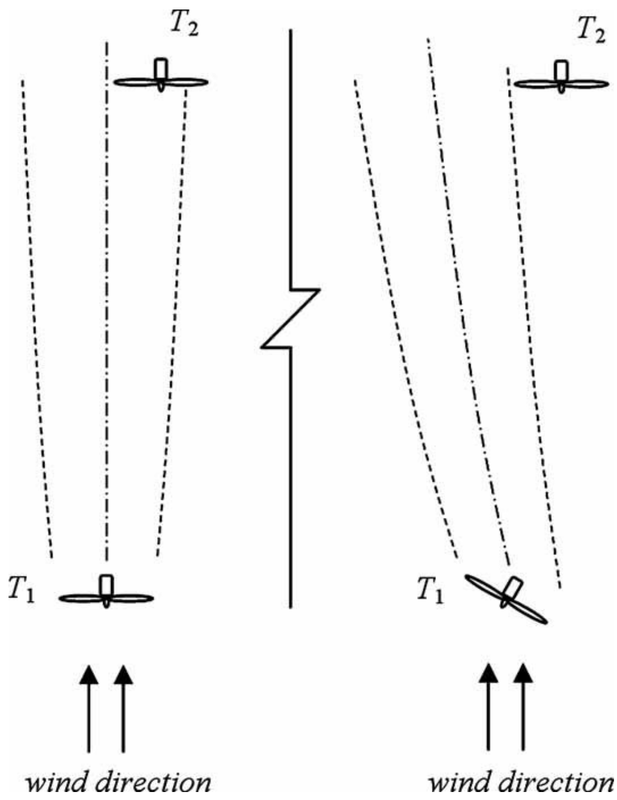

Figure 1. Wake deflection due to yaw control of a turbine [13]

2.2 Theoretical foundation

This section describes the theoretical methods used in chapter 2. Wake models in general and the used wake model in detail are described in subsection 2.2.1. In subsection 2.2.2 an overview of optimization methods is given and in subsection 2.2.3 the used optimization tools OpenMDAO and WISDEM are explained.

2.2.1 Wake model

In general, the wake of a turbine can be divided in two regions: the near wake and the far wake. For onshore conditions the near wake is the region 2-3 rotor diameters down-stream from the turbine where the flow field is mainly affected by the rotor shape whereas in the far wake region, i.e. 3-5 rotor diameters downstream from the turbine, the influence of the rotor shape can be neglected. Because of diffusion effects, the extension of the near and far wake region is dependent on the ambient turbulence and differs under offshore conditions. In the far wake the influence of wake interactions, turbulence or topographic effects are more important than in the near wake. From a simplified point of view, the flow field within the wake is a result of wind shear, wind speed deficit and turbulence (see Figure 2).

The wind speed deficit occurs through the rotor extracting energy from the wind. The deficit reaches its maximum in the near wake and recovers with sufficiently distance from the turbine because of

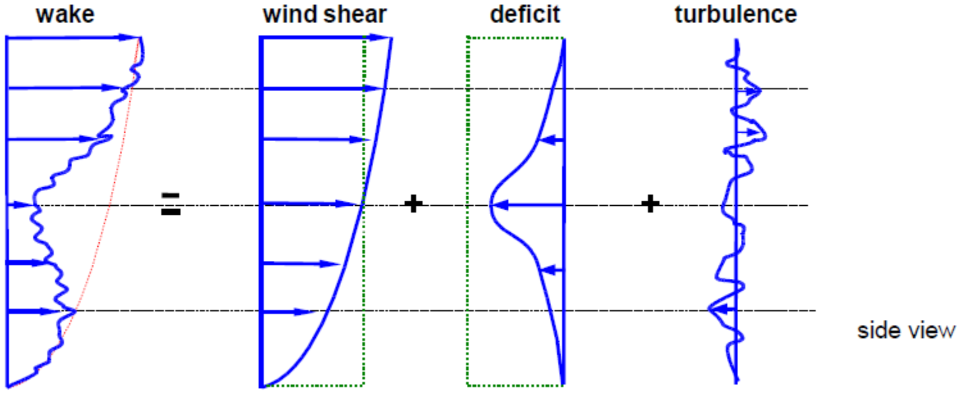

Figure 2. Resulting flow field in the wake [2]

turbulent diffusion of the wake [22]. The qualitative change of the wind speed deficit is shown in Figure 2. The shape of the wind speed deficit and the expansion of the wake is modelled differently for each wake model being used.

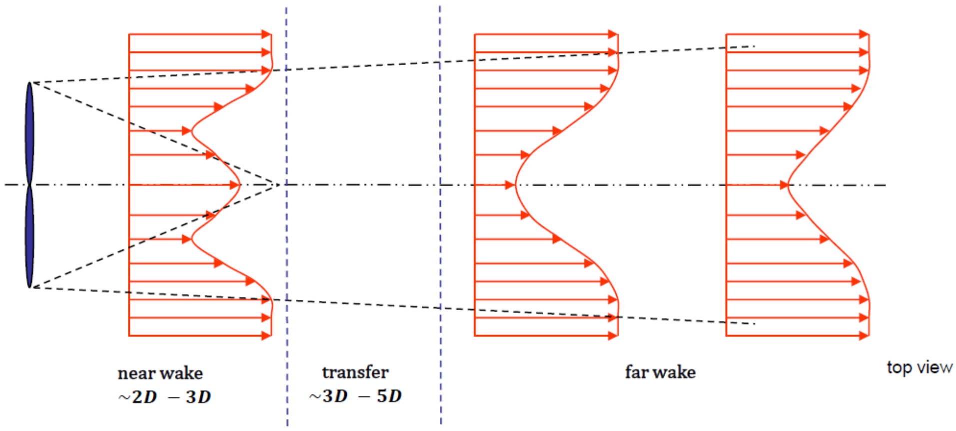

Figure 3. Qualitative change of wind speed deficit in the wake [2]

In a wind farm there is the possibility that one turbine is standing in the wake of one or more turbines. For example, in Figure 4, turbine 7 has an incoming inflow wind speed reduced by the wakes of turbine 1 and 4 resulting in a lower power production. In wind farm layout optimization, because of the turbines rarely being placed in the near wake, the far wake is from greater importance [25].

The wake model used in this chapter is FLORIS. FLORIS is a parametric wind turbine wake model that was developed for optimizing the yaw settings and turbine locations [10, 23, 17]. FLORIS is a combination of Jensen's wake model and a model for wake deflection through yaw [13]. For improving the physically accuracy, the FLORIS model developed in [10] defines three different wake zones (shown in Figure 5): near wake, far wake and mixing zone. Each wake contains unique parameters for wake decay and velocity deficit. The parameters for each wake zone were obtained by LES simulations in SOWFA [10].

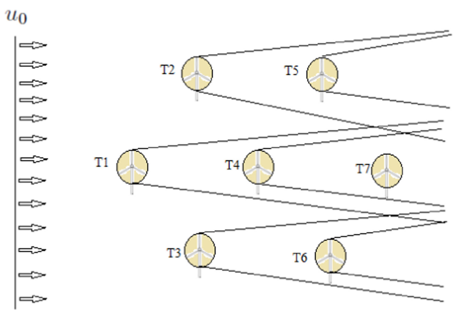

Figure 4. Multiple wakes in a wind farm [22]

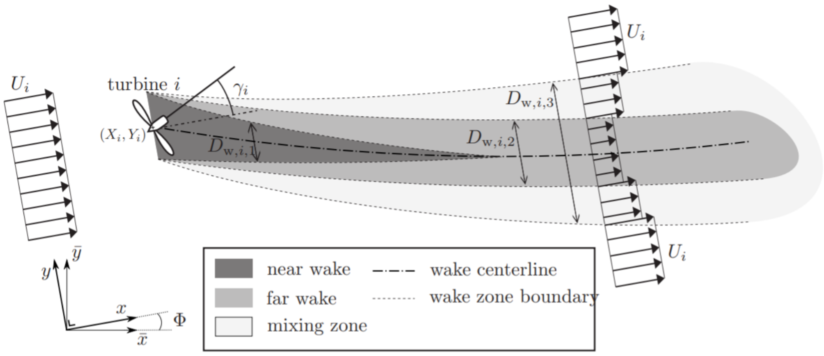

Figure 5. Different wake zones of FLORIS and wake deflection (top view) [24]

The diameter of the respective wake zone q is given by:

$$D_{w,j,q}(x) = \max(D + 2k_e m_{e,q} x, 0)\,. \tag{2.1}$$

The wind speed in the wake in zone is defined as:

$$V_{w,q} = V_\infty \times \Big(1 - 2ac_q(x,r)\Big)\,, \tag{2.2}$$

in which the variables are defined in Table 1:

Variable	Definition
$D_{w,j,q}(x)$	Diameter of the wake in zone q caused by turbine j
D	Turbine diameter
k_e	Wake expansion parameter
$m_{e,q}$	Wake expansion parameter in wake zone q
$V_{w,q}$	Wind speed in the wake in wake zone q
V_∞	Undisturbed wind speed
a	Idealized induction factor $a = 1/3$
c_q	Wake decay coefficient in zone q
x	Distance behind turbine
r	Radial distance from the center of the wake

Table 1. Definitions of FLORIS parameters

The normalized wind speed deficit is then calculated to:

$$\frac{\Delta V}{V_\infty} = \frac{V_\infty - V_\infty \times \Big(1 - 2ac_q(x,r)\Big)}{V_\infty} = 1 - 2ac(x,r)\,. \tag{2.3}$$

The following applies for the wake decay coefficient in zone q:

$$c_q(x,r) = \begin{cases} c_1 & r \leq \frac{D_{w,1}}{2} \\ c_2 & \frac{D_{w,1}}{2} \leq r \leq \frac{D_{w,2}}{2} \\ c_3 & \frac{D_{w,2}}{2} \leq r \leq \frac{D_{w,3}}{2} \\ 0 & r > \frac{D_{w,3}}{2}\,. \end{cases} \tag{2.4}$$

The wake decay coefficient for each turbine j can be obtained by:

$$c_j = \left(\frac{D}{D + 2k_e m_{U,q}(\gamma) x}\right)^2, \tag{2.5}$$

where $m_{U,q}(\gamma)$ is an empirically adjustment to the wake decay rates considering the rotor yaw angle γ with the velocity parameters $M_{U,q}$, a_u and b_u in the wake zone q:

$$m_{U,q} = \frac{M_{U,q}}{\cos(a_U + b_U\gamma)}\,. \tag{2.6}$$

The steady state power P of the turbine is calculated by:

$$P = \frac{1}{2}\rho A_{\text{Turbine}} c_p(a,\gamma) V_\infty\,. \tag{2.7}$$

To account for other losses and for correcting the influence of the yaw angle, the power coefficient c_p is computed by:

$$c_p(a,\gamma) = 4a(1-a)^2 \eta \cos(\gamma)^{pP}\,, \tag{2.8}$$

with turbine power correction factors pP and η.

Turbine Power	wake	
	Expansion	velocity
$\eta = 0.77$	$k_e = 0.05$	$M_{U,1} = 0.5$
$c_p = 1.88$	$m_{e,1} = -0.5$	$M_{U,2} = 1.0$
	$m_{e,2} = 0.22$	$M_{U,3} = 5.5$
	$m_{e,3} = 1$	$a_U = 12.0$
		$b_U = 1.3$

Table 2. Parameters for FLORIS (From [9])

2.2.2 Optimization methods

In general, optimization is the finding of the minimum or maximum of numbers, functions, or systems [14]. Each optimization problem consists of the same fundamental structure: minimize/maximize an objective function by varying one or more design variables (parameters). The permitted value of a parameter can be restricted by constraints. There are two types of constraints: equality or inequality constraints. Equality constraints state that a functional relationship between one or more parameters equals a specific value. Inequality constraints state that the functional value of the parameters has to be either greater than or smaller than a specific value.

There are two different types of extreme: local and global extreme. In Figure 6 both local and global minimum of the objective function $f(x)$ are shown. If there is no point with a smaller/greater function value in the region of the minimum/maximum, it is a local minimum/maximum. A global minimum/maximum is the smallest/greatest feasible function value in the entire search space.

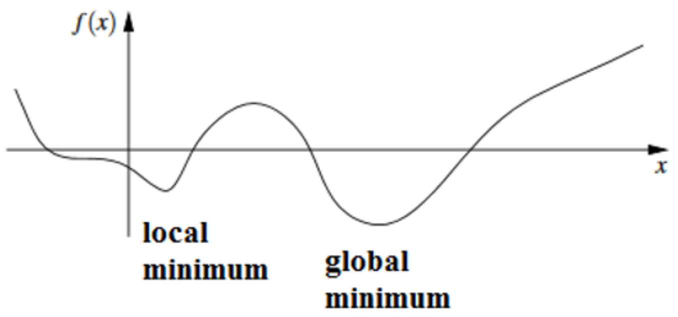

Figure 6. Local and global minimum of the function $f(x)$ [20]

Local optimization is the search for a local optimum and the algorithms used for local optimization are usually fast, but they do not always find the best solution. Global optimization problems may possess one or more local optima which are not globally optima, therefore the global optimum is more difficult to obtain [29].

If both the objective function and the constraints are linear functions of x, the optimization problem is a linear programming problem. If at least one function is nonlinear then it is a nonlinear programming problem. In convex programming, all local optima are also global optima. Linear programming problems belong to the category of convex programming.

Optimization algorithms are iterative. They start from an initial point - in wind farm layout optimization the initial Layout - and estimate the optimal solutions for the design variables. In the next iteration an improved estimation of the design variables is made. The manner of how to find a better solution between each iteration is what distinguishes the different optimization algorithms [29]. The properties of a good optimization algorithm are robustness, efficiency and accuracy. These properties may stand in direct conflict to each other which make a good compromise necessary.

In this chapter, the objective function is AEP and the optimization parameters are the x and y position within the wind farm as well as yaw misalignment of turbines. Constraints are the available area of the wind farm and the minimal distance between each turbine.

2.2.3 Optimization tools

2.2.3.1 openMDAO

OpenMDAO (Multidisciplinary Analysis and Optimization) is an open-source high performance computing platform for systems analysis and multidisciplinary optimization, written in python [18]. The development of OpenMDAO is supported by the NASA Glenn Research Center with the purpose of fostering unconventional aircraft concepts, but the framework is general and not linked to a specific discipline. Because of the efficient and accurate computation of the derivatives, the platform is focused on supporting gradient based optimization with analytical derivatives enabling the examination of optimization problems with thousands of design variables. Nonetheless, OpenMDAO also provides gradient-free optimization, mixed-integer nonlinear programming and traditional design space exploration. Detailed information on OpenMDAO can be found in [11].

The main elements in OpenMDAO are called Components and Drivers. A Component is an object with input and output variables. Within Components calculations are executed. The task of the driver is to iterate over a workflow. In the simplest case a driver iterates over a workflow only once but an optimization driver usually iterates multiple times over a workflow until an abort criterion is reached. All these elements are structured in an Assembly (see Figure 7). In the Assembly the workflow and the connections between each component are defined. Also, the optimization objective, parameters and the constraints are defined in the Assembly.

In OpenMDAO different kinds of optimization algorithms are available and displayed in Figure 8. The algorithms differ in the capability of calculating their own gradient via finite difference or the ability of handling inequality and/or equality constraints. The optimization algorithm used in this chapter is SLSQP (Sequential Least SQuares Programming) provided within OpenMDAO [18]. It is a nonlinear, gradient-based algorithm which is able to handle inequality constraints. Iterations are generated by solving quadratic sub-problems. Further information on Sequential Quadratic Programming Methods can be found in [29, 21, 12].

2.2.3.2 WISDEM

The Wind-Plant Integrated System Design and Engineering Model (WISDEM) is a set of models for assessing overall wind plant cost of energy. It is built in OpenMDAO and uses several sub-models that are also designed as OpenMDAO plug-ins. These sub-models can be used independently but they are required to use the overall WISDEM capability [28]. WISDEM includes integrated assemblies for the assessment of system behavior of wind turbines and plants [6]. For research on optimizing the layout of a wind farm the variables in these assemblies can be declared as design variables. The general software framework of WISDEM is shown in Figure 9 . OpenMDAO is responsible for a

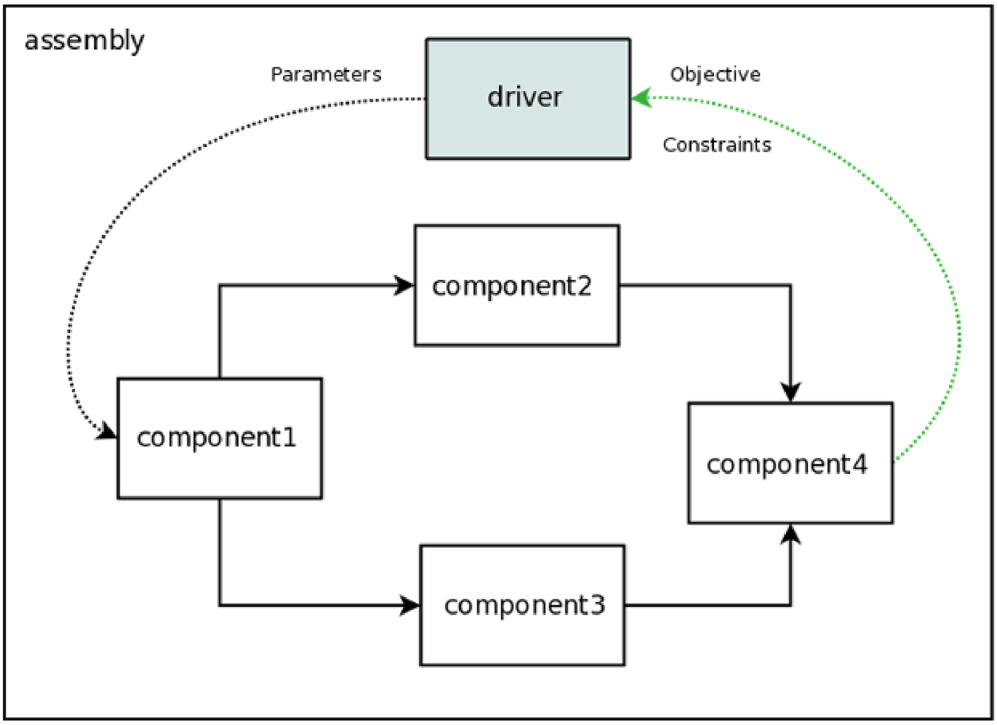

Figure 7. General data flow in OpenMDAO [19]

Optimizer	Gradients	Inequality Constraints	Equality Constraints	Algorithm
COBYLAdriver	None	Yes	No	Constrained Optimization BY Linear Approximation of the objective and constraint functions via linear interpolation
CONMINdriver	Computed by OpenMDAO or CONMIN	Yes	No	CONstrained function MINimization. Implements the Method of Feasible Directions to solve the NLP problem
Genetic	None	No	No	General genetic algorithm framework based on PyEvolve
NEWSUMTdriver	Computed by OpenMDAO or NEWSUMT	Yes	No	NEWton's method Sequence of Unconstrained Minimizations
SLSQPdriver	Computed by OpenMDAO	Yes	Yes	Sequential Least SQuares Programming

Figure 8. Available optimization algorithms in OpenMDAO 0.13.0 [18]

structured workflow of the different models used in WISDEM, FUSED-Wind (Framework for Unified Systems Engineering and Design of Wind Plants) provides a joint platform for different simulation codes. The different analysis tools of WISDEM are integrated into FUSED-Wind and OpenMDAO. In this chapter, the plugin FLORIS-SE is used. It provides a simplified version of the WISDEM FLORIS model based on the structure of OpenMDAO.

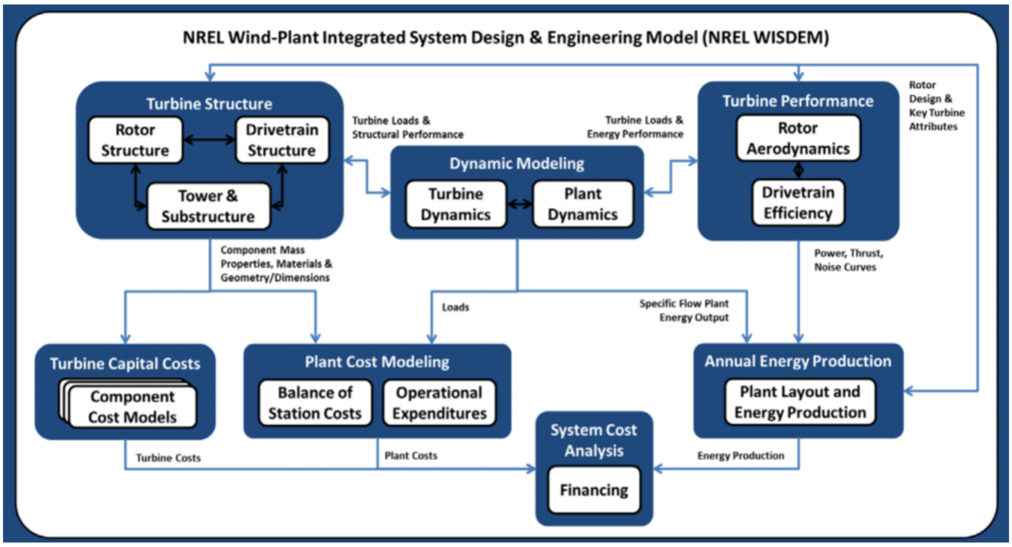

Figure 9. Software framework of WISDEM [7]

2.3 Problem definition and goals

The aim in this chapter is to investigate the possibilities of yaw and layout optimization using WISDEM as optimization tool. The optimized wind farm is the NORCOWE reference wind farm [16]. The placing of the turbines is shown in Figure 11. The available wind farm area is limited by a rectangular boundary. The boundary was chosen because there are no further adaptions to the code necessary as only a lower and upper limit of the X and Y position of the turbines has to be defined. Further investigations could consider other boundaries like a circular boundary or a much narrower rectangular boundary.

For the optimization, measurement data from FINO3 [8] for the years 2000-2010 is used. As a first step, the measurement data was binned in six wind directions. For each wind directions, the average wind speed and the probability of occurrence was determined. The used wind directions with belonging frequency and average wind speed are listed in Table 3 and shown in a wind rose pictured in Figure 12a.

The low number of wind directions was mainly chosen because of time considerations as an optimization of turbine positions with 82 turbines and 6 wind directions lasts about 48 hours. The wind rose for a 12 wind directions scenario is plotted in Figure 12b. Different quantitative, but not qualitative results are expected for considering different number of wind direction. We believe this depends mainly on the probability distribution of wind directions. For a reduced number of wind direction if

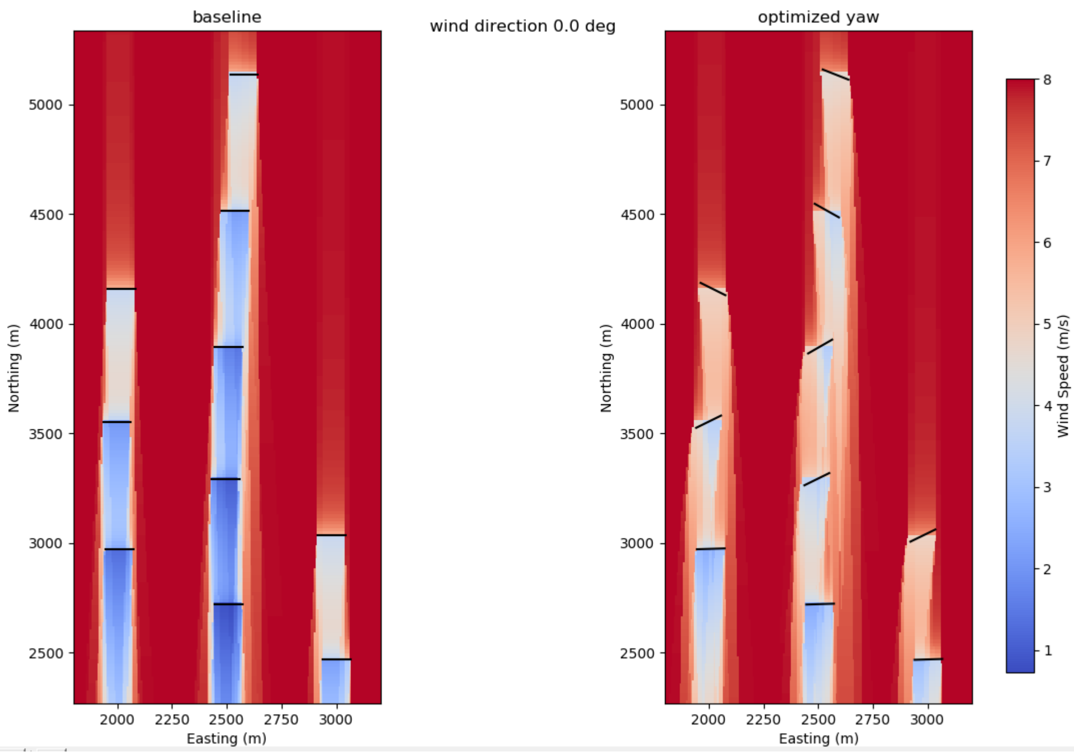

Figure 10. Yaw optimization for a subset of 10 turbines in FLORIS-SE

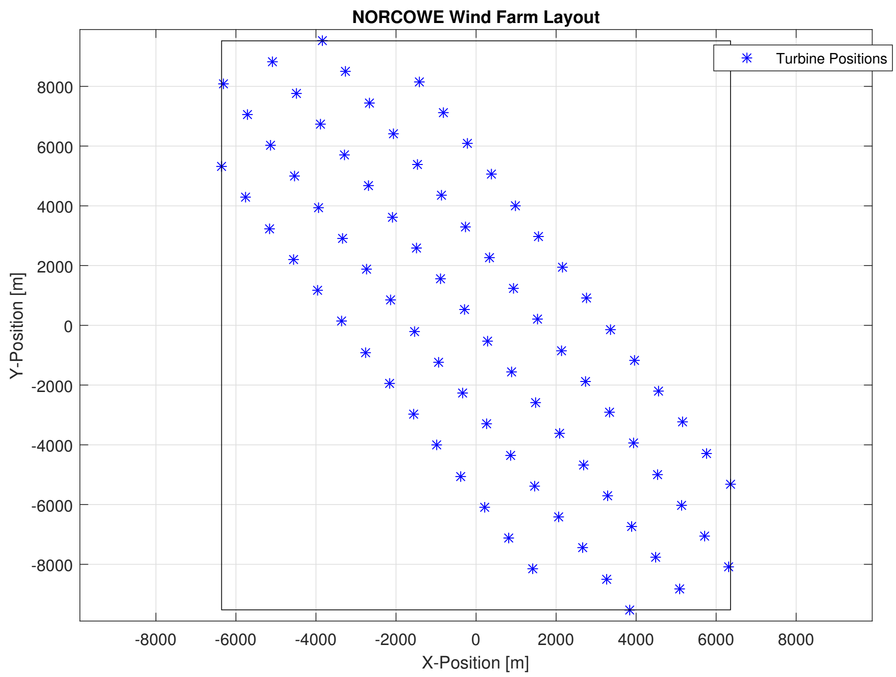

Figure 11. NORCOWE wind farm layout with rectangular boundary

Wind direction	Frequency [%]	Average wind speed [m/s]
30°	13.36	9.40
90° (East)	8.96	7.74
150°	18.29	9.65
210°	23.85	10.51
270°(West)	21.53	11.19
330°	14.02	9.86

Table 3. Wind direction, frequency and average wind speed for 6 wind directions

(a) Wind rose with 6 wind directions **(b) Wind rose with 12 wind directions**

Figure 12. Wind Roses from FINO 3 (the code in [27] is used)

the prevailing wind directions are omitted this could lead to a considerable difference between the optimization results.

The main objective of the optimization is to maximize the AEP of the wind farm with given restrictions. The AEP is generally defined as:

$$\text{AEP} = (\sum_{i=1}^{16} f_i \times P_i)8760\,, \tag{2.9}$$

where i stands for i^{th} wind direction and P_i and f_i are produced power and wind direction probability for i^{th} wind direction, respectively.

In case of position optimization, the design variables are the X and Y position of each turbine of the wind farm, limited by the constraint that the turbines have to be placed inside the rectangular boundary. Another constraint is the minimum distance between any two turbines which is equal to two rotor diameters. In case of yaw optimization, the design variable is the yaw angle of each turbine with a lower limit of -30° and an upper limit of $+30^\circ$. In the case of combined optimization, the design variables of position and yaw optimization are taken into account.

The turbine used in this chapter is the DTU 10MW RWT with the following characteristics shown in Table 4 [1]:

Rotor diameter	178.3 m
Turbine rating	10 MW
Cut-In wind speed	4 m/s
Rated wind speed	11.4 m/s
Cut-Out wind speed	25 m/s
Hub height	119.0 m

Table 4. DTU 10MW Wind turbine characteristics

Wind speed [m/s]	C_P	C_T	Wind speed [m/s]	C_P	C_T
4	0.286	0.923	15	0.207	0.259
5	0.418	0.919	16	0.170	0.211
6	0.464	0.904	17	0.142	0.175
7	0.478	0.858	18	0.119	0.148
8	0.476	0.814	19	0.102	0.126
9	0.476	0.814	20	0.087	0.109
10	0.476	0.814	21	0.075	0.095
11	0.476	0.814	22	0.065	0.084
12	0.402	0.557	23	0.057	0.074
13	0.317	0.419	24	0.050	0.066
14	0.253	0.323	25	0.044	0.059

Table 5. Values for C_P and C_T of the DTU 10MW RWT [1]

2.4 Realization of the optimization

In WISDEM, the plugin FLORIS-SE provides a possibility for layout and/or yaw optimization using FLORIS as wake model, but under consideration of only one wind direction. The workflow of FLORIS-SE had to be changed to consider the wind directions defined in this chapter. The adapted workflow of FLORIS-SE is shown in Figure 13.

2.4.1 Adapting FLORIS-SE

FLORIS consists of 6 components which are handled by two different drivers. A special point in FLORIS is the ability to consider wake phenomena caused by wake deflection and yaw misalignment. The calculation of the influence on the C_P and C_T values for each turbine takes place in the component “Calculate C_P and C_T Depending on Yaw” (see Figure 13). The values are handed over to the other components by the Fixed-Point Iterator. Inputs of FLORIS-SE are the Initial Layout, turbine data (C_P and C_T values for each wind direction, hub height and rotor diameter) and the wind rose containing wind directions, wind speed and probability for each wind direction

The calculation of the wind farm AEP is executed for each wind direction separately. Therefore, a coordinate transformation takes place in the component “Wind Frame”, where the layout of the wind farm is rotated according to the actual wind direction enabling the wake calculations for each wind direction. The calculation of the different wake zones, the wake losses and the calculation of partial

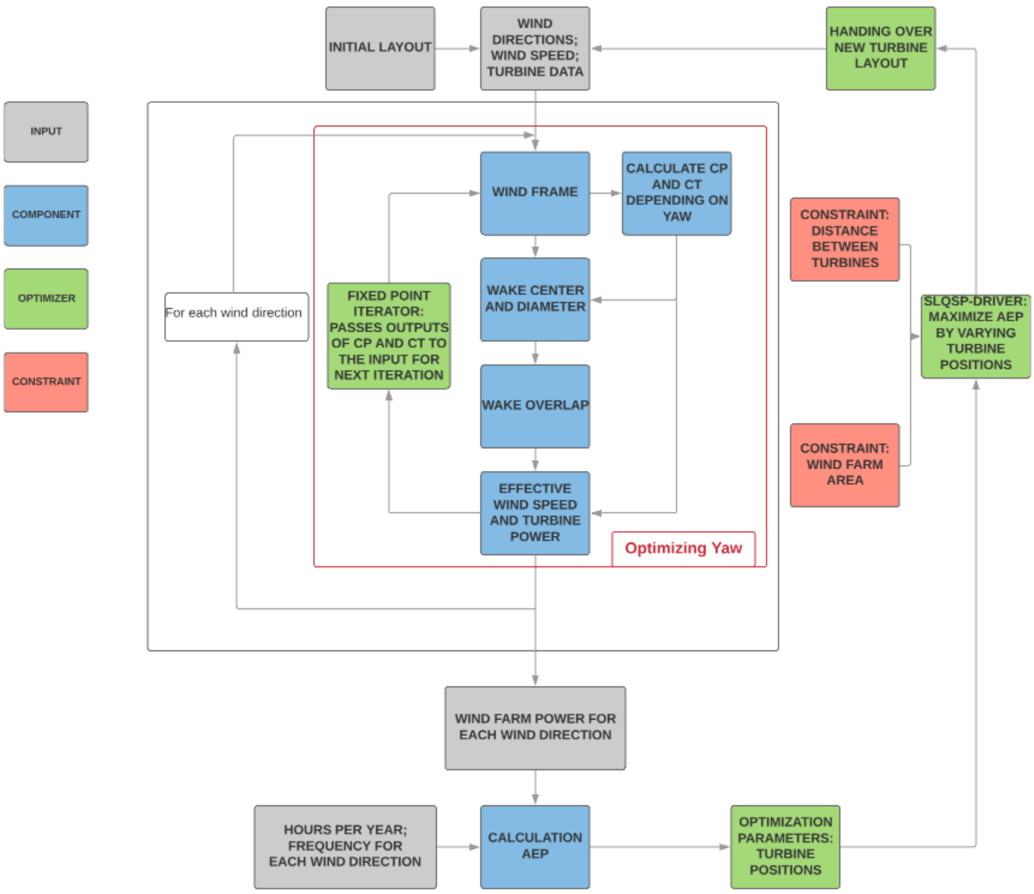

Figure 13. Adapted workflow of FLORIS-SE

and multiple wake takes place in the components “Wake Center and Diameter”, “Wake Overlap” and “Effective wind speed and turbine power”. In the component “Calculation AEP” the energy production for each wind direction is then weighted with its corresponding frequency and summarized to obtain the total energy production of the wind farm. In addition, the component “Calculation AEP” contains the objective function and therefore the driver “SLSQP” tries to maximize it while iterating through the workflow. The parameters of the X and Y turbine position are limited by the two constrains “Distance between Turbines” and “Wind Farm Area”.

2.4.1.1 Implementation of the wind rose

In the original version of FLORIS-SE it is possible to integrate a wind rose, but the optimization was executed for each particular wind direction resulting in different optimized layouts for each wind direction. Therefore, it was necessary to remove a FOR-loop in the input file which handed over each wind direction separately. Instead, new arrays containing the wind directions and the related wind frequencies and wind speeds were created. The wind data is read in from a MATLAB file. In addition to this, the parameter defining the number of considered wind directions and wind speeds had to be set up to match the size of the arrays.

2.4.1.2 Initial layout

The initial layout used in FLORIS-SE is based on the Princess Amalia wind farm. The layout is read in through a MATLAB file. There is the possibility to use either a subset or all turbines of the wind farm. For using self-created initial layouts, the MATLAB file has to be replaced by another file containing the desired turbine locations of the NORCOWE wind farm. The turbine locations are handed over using two vectors called *turbineX* and *turbineY*.

2.4.1.3 Implementing the DTU 10MW RWT

In the original version of FLORIS-SE the used turbine is the NREL5MW reference turbine. Rotor diameter and hub height are originally defined in the Input file, the values for C_P and C_T are read in from a separate file. To implement the DTU 10MW RWT, a MATLAB file containing the necessary turbine data was created. The data from the MATLAB file is now read in directly. If future optimizations are going to be carried out with another turbine, the MATLAB file has to be replaced with the turbine data of the new turbine.

2.4.2 Troubleshooting

Position and yaw Optimizations considering 82 turbines and 6 wind directions were carried out successfully. In the case of combined optimization, an error appeared when using more than 59 turbines and 6 wind directions. When using 60 turbines, OpenMDAO displays the following error: “RuntimeError: driver: Numerical overflow in the objective”. The error could not be eliminated as the problem appears to be in the code of OpenMDAO not being able to handle a certain number of parameters.

Number of turbines	Number of directions	Optimization case	Error
59	6	Combined	No
59	12	Combined	No
60	6	Combined	Yes
60	12	Combined	No
65	6	Combined	No
65	12	Combined	No
70	6	Combined	Yes
70	12	Combined	Yes
82	6	Position	No
82	6	Yaw	No

Table 6. Troubleshooting with different number of turbines and wind directions

Optimization case	Initial AEP [GWh]	Optimized AEP [GWh]	Improvement of AEP [GWh]	Computational time [hours]
Position-Only	3752.3	5027.4	1275.1 (+33.98%)	47.3
Yaw-only	3752.3	4067.0	314.7 (+ 8.39%)	35.7
Combined	3752.3	5029.1	1276.8 (+34.02%)	47.3+34.3

Table 7. Optimization results for the different optimization cases

In a combined optimization OpenMDAO has to consider the parameters X position, Y position, yaw angle of each turbine, constraints for each parameter and additionally the distance constraint of two rotor diameters. Strangely enough, when increasing the number of turbines or the number of wind directions in some cases the error did not appear. In Table 6 a short overview of the different scenarios is given.

To obtain a result for a combination of position and yaw optimization considering 82 turbines, a layout optimization was carried out. The obtained optimized layout was then yaw optimized.

2.5 Results and discussion

In this section the results of the different optimization cases are shown. In Figure 14 both the initial NORCOWE (blue) and the optimized (red) layout are shown. The optimized layout is used in the combined optimization as initial layout for yaw optimization. All optimizations were carried out using 6 wind directions. Due to the great available wind farm area, the change of turbine position is significant. The turbines are -like in the initial layout- placed in rows, but with a greater distance in between them.

The optimization results of the different optimization cases are listed in Table 7. The best optimization result is achieved by combined optimization with a 34.02% improvement of AEP. . However, the position-only optimization achieves just a slightly worse result with 33.98% and a much shorter computational time. The improvement in the yaw-only optimization is 8.39% while having the shortest computational time. Considering Table 8, in which the yaw angles of the yaw-only and the combined

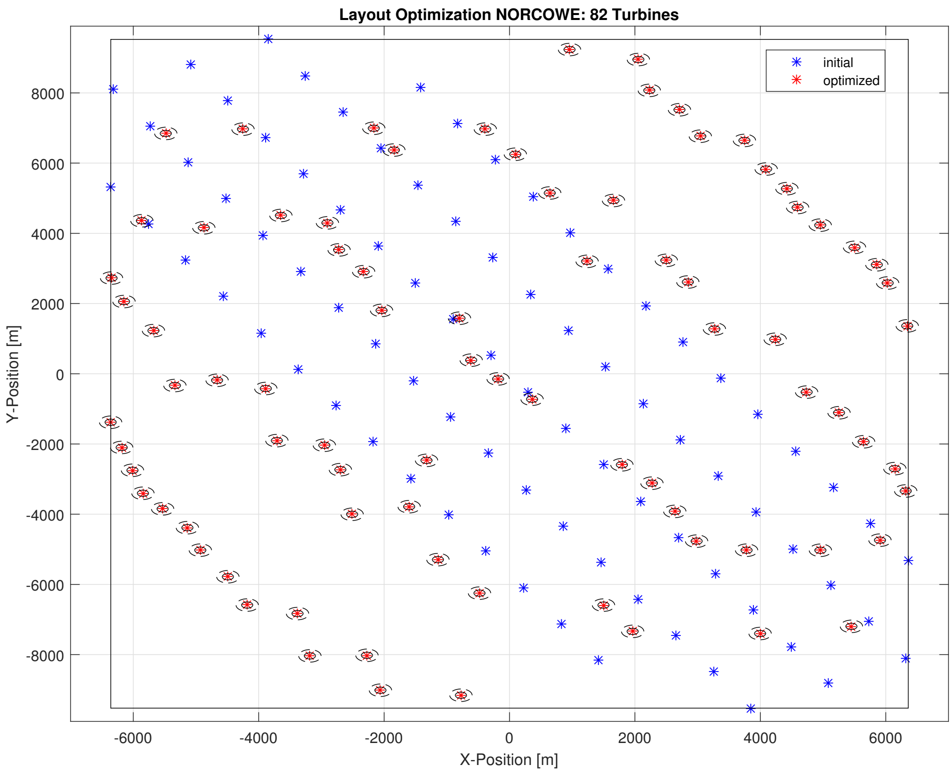

Figure 14. Position-optimized NORCOWE

	Yaw-Only		Combined	
Wind direction	Average yaw angle	Maximum yaw angle	Average yaw angle	Maximum yaw angle
$0°$ (North)	$7.6°$	$13.7°$	$0.9°$	$5.7°$
$60°$ (N-E)	$20.0°$	$26.4°$	$0.5°$	$2.8°$
$120°$ (S-E)	$10.4°$	$15.0°$	$0.6°$	$4.3°$
$180°(South)$	$8.1°$	$13.3°$	$1.1°$	$5.7°$
$240°$ (S-W)	19.8	$26.6°$	$0.5°$	$2.4°$
$300°$ (N-W)	$10.4°$	$14.8°$	$0.5°$	$3.5°$

Table 8. Yaw angles for each wind direction $Combinedoptimization$

optimization cases are listed, the following can be concluded:

- With a great available wind farm area, the improvement of AEP is the highest when optimizing the position of the turbines.
- Yaw optimization is expected to be more important in a wind farm in which the turbines are placed with less distance between each other.
- In the optimized layout, where the turbines are placed far apart from each other, yaw optimization has nearly no influence on the optimization result and therefore the average yaw angle of the turbines is much smaller than in the NORCOWE layout.
- Yaw optimization is faster than position optimization.

3 WIND FARM REDESIGN USING INDUCTION CONTROL ONLY

This section investigate the impact of induction control only on farm layout. New results indicate induction control only will not work at all. The implications of this is first discussed. The conclusion is that the Economic Model Predictive Controller (EMPC) and probably any induction based controller will not change the farm geometry. Therefore it does not make sense to perform a detailed investigation and simulation to verify this. However, a smaller investigation is made to find an upper limit to the amount a farm could be squeeze under ideal conditions where the mean wind speed is at an ideal value below rated.

3.1 New results on induction control

Early results on induction wind farm control showed power performance increase in the range 2-6% typically under ideal static conditions [15]. Already when the data driven EMPC method was developed it was known that it would be hard to improve on power performance.

After the development of the EMPC control method new results has questioned the success for induction control only even more. Under ideal static conditions Deliverable D4.2 [4] section 5 showed a power increase of 1% based on SimWindFarm simulations of the 9 WT CLWindcon farm in Deliverable D1.1 [3]. This was obtained using small relative derating not exceeding 0.038.

In the paper [5] in Deliverable D2.3 a solution including both wake steering and induction control was investigated. The conclusion there was that it was optimal to not derate at all. Deliverable D2.3 section 5.2.2 concludes that there is nothing, or in the best case very little e.g. 0.2%, to win with only induction control. Further, section 5.2.3 states “In the remainder of this European project, induction control will be tested in combination with wake redirection control..”.

These new results suggests that it is not worth to conduct a large investigation on induction control only. The investigation in Deliverable D3.5 verified that this is the case for the EMPC controller in Deliverable D2.3.

3.2 Approach

As discussed above in section 3.1 the latest results shows very limited potentials for induction control only. Therefore this section describes a simplified approach to find a upper bound for the impact on farm design.

In wind farm design the two most important KPI’s are farm power and fatigue in that order. If these were the only KPI’s wind farms would be much larger in area. Because of wake effects approximately 5-10% [15] power is lost in today’s wind farm compared to the turbines standing “alone” with very large inter turbine distance. The reason for denser farms is that there are cost increasing with the inter turbine distance and the farm area. These farm size cost are e.g. cabling, operation and maintenance, and installation. In practice many other costs related factors or regulations must be accounted for in wind farm design. These include water depth, seabed conditions, endangered species, fishery, sea transport etc. Clearly, it is difficult to include sufficient cost components to cover a real wind farm design. However, the farm size can be used as a proxy for the most important costs discussed above.

The above leads to the following two questions that will be investigated here:

- Can the farm be squeezed by a small length scale factor with less degradation in power and fatigue using induction only farm control compared to no (greedy) control?
- How much can a farm be squeezed before the induction only controller can not make up for the reduction in power and/or fatigue compared to no control.

The answers will be based on a simplified analysis under ideal conditions which then gives a upper bound for the result. The conditions are the following: wind farm is the 3x3 CLWindcon wind farm from Deliverable D1.1 [3]. Only one mean wind speed at 8 m/s and turbulence intensity 0.1 will be used. The direction is assumed uniform distributed over all directions. The controller will be the feed forward (FF) controller described in Deliverable D4.2 [4] section 5.1 which is based on a analytic optimization using the static Jensen model. SimWindFarm will be used for simulation. It would also be of interest to see results for the “Norcowe” wind farm described in Deliverable D1.1 [3]. However, this wind farm has 88 turbines which is to many for dynamic simulation with SimWindFarm.

3.3 Upper limit to squeezing a wind farm using induction control only

First some results based on the Jensen model are derived. They gives suggestion for how much the farm can be squeezed without loosing performance. This is then used for the SimWindFarm time simulation.

3.3.1 Analysis based on Jensen model

Using the simple Jensen wake model for one row of turbines it is possible to maximize the farm (row) power using dynamic programming which turns a multi dimensional optimization into a sequence of one dimensional optimizations. In Deliverable D4.2 [4] section 5.1 this method is developed and explained in details. This is used here to obtain the optimal induction $a_i, i = 1, \ldots, n$ for each turbine in the n turbine row. Using the disc actuator model both C_p and C_t is given by the induction and with the Jensen wake model the local wind turbine wind speeds v_i are given by the inductions and the ambient wind speed v_a. This leads to the following definition of a row power coefficient $C_{p,r}$ and thrust coefficient $C_{t,r}$ as follows:

$$P_r = \sum_{i=1}^{n} P_i = \sum_{i=1}^{n} \frac{1}{2}\rho A v_i^3 C_p(a_i) \triangleq n\frac{1}{2}\rho A v_a^3 C_{p,r} \Leftrightarrow \tag{3.1a}$$

$$C_{p,r} = \frac{1}{n}\sum_{i=1}^{n}\left(\frac{v_i}{v_a}\right)^3 C_p(a_i) \tag{3.1b}$$

$$T_r = \sum_{i=1}^{n} T_i = \sum_{i=1}^{n}\frac{1}{2}\rho A v_i^2 C_t(a_i) \triangleq n\frac{1}{2}\rho A v_a^2 C_{t,r} \Leftrightarrow \tag{3.1c}$$

$$C_{t,r} = \frac{1}{n}\sum_{i=1}^{n}\left(\frac{v_i}{v_a}\right)^2 C_t(a_i) \tag{3.1d}$$

The above equations (3.1) shows that $C_{p,r}$ (3.1b) and $C_{t,r}$ (3.1d) can be interpreted as average row (farm) power and thrust coefficient with respect to the ambient wind speed v_a. The row performance expressed by $C_{t,r}$ and $C_{p,r}$ can be calculated for both optimal and greedy operation with $a_i = 1/3, i = 1, \ldots, n$. This is done for inter turbine distances from 4 to 9 diameters. This is a normal range for real wind farms. Moreover it also covers the 3x3 CLWindcon farm with distances 5, 7, $\sqrt{5^2+7^2}$= 8.60. The plots of this is shown in figure 15.

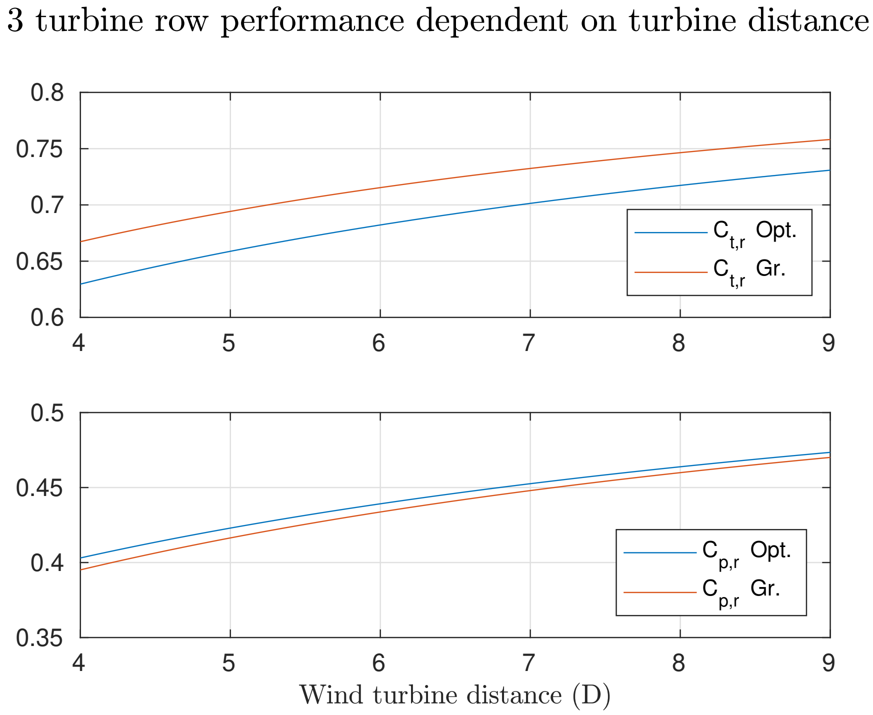

Figure 15. Turbine row performance dependent on turbine distance. $C_{p,r}$ (3.1b) and $C_{t,r}$ (3.1d) are defined in (3.1). Opt. are for optimal operation and Gr. mean greedy i.e. standard operation.

Both average power and thrust coefficient increase with inter turbine distance as the wind speed at down wind turbines increases with distance. As the average power coefficient curve for optimal operation is above the one for greedy operation it is possible to squeeze the distance a small amount when changing from greedy to optimal operation and still get the same power. This is shown in table 9. The first row is the average coefficient for a inter turbine distance of 6. The distance in the second row is found numerically as the smallest distance where $C_{p,r}$ for optimal operation is at least as large as for greedy operation at distance 6D. According to this the row can be squeezed with a factor $5.65/6 = 0.9417$ without loosing power. For this squeezing the Average $C_{t,r}$ relative change is ($C_{t,r}$ Opt. D= 5.65/$C_{t,r}$ Gr. D= 6) $0.6745/0.7154 = 0.9428$. Reduced average thrust indicate reduced tower load as smaller average load normally gives smaller variations which in turn gives smaller fatigue. In short: changing from greedy to optimal operation the farm can be squeezed by 6% with no loss of power and with 6% reduction of thrust.

D	$C_{t,r}$ Opt.	$C_{p,r}$ Opt.	$C_{t,r}$ Gr.	$C_{p,r}$ Gr.
6	0.6822	0.4392	0.7154	0.4337
5.65	0.6745	0.4339	0.7085	0.4280

Table 9. Turbine row performance dependent on turbine distance.

3.3.2 Dynamic time simulation results using SimWindFarm

For the time simulations the 3x3 CLWindcon wind farm with the geometry shown in figure 16 is used. Mean wind speed 8 m/s and turbulence intensity 0.1 is used for all simulations. Four wind directions 0, 30, 60, 90 degrees are used. The final results will be the average over these wind directions. For direction 0 and 90 degrees the wind direction is along the row/columns of turbines.

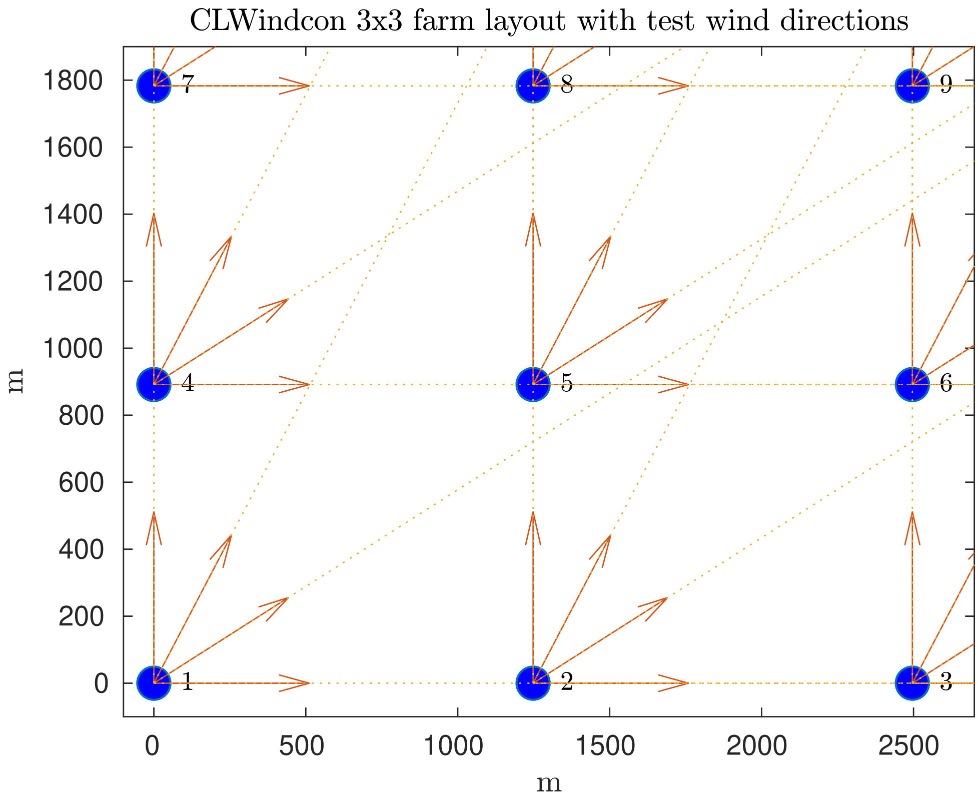

Figure 16. CLWindcon 3x3 farm layout with test wind directions.

The FF deratings calculated by the Jensen wake model (Deliverable D4.2 [4]) for one row can then be directly used. Direction 30 degrees is sufficiently close to the diagonal direction to use the deratings corresponding to this. For direction 60 degrees only the wake from turbine 1 to 8 and 2 to 9 are considered significant. The deratings for turbine 1 and 9 is then calculated as for a two turbine row with distance $\sqrt{(7D)^2 + (10D)^2}$. The deratings are shown for all 4 directions in table 10.

Wind	Turbine number								
direction	1	2	3	4	5	6	7	8	9
0	0.025	0.007	0	0.025	0.007	0	0.025	0.007	0
30	0.019	0.005	0	0.005	0.005	0	0	0	0
60	0.003	0.003	0	0	0	0	0	0	0
90	0.038	0.038	0.038	0.010	0.010	0.010	0	0	0

Table 10. Derating settings for the turbines when running with optimal deratings calculated from the Jensen wake model as explaned in Deliverable D4.2 [4]. See text for further details.

One example of the time series for a simulation is shown in figure 17. As seen in the shown signals, especially the wake deficit, it takes some time before the initial conditions has died out. Therefore the results are only based on the last 600 seconds of the 1200 seconds simulation time.

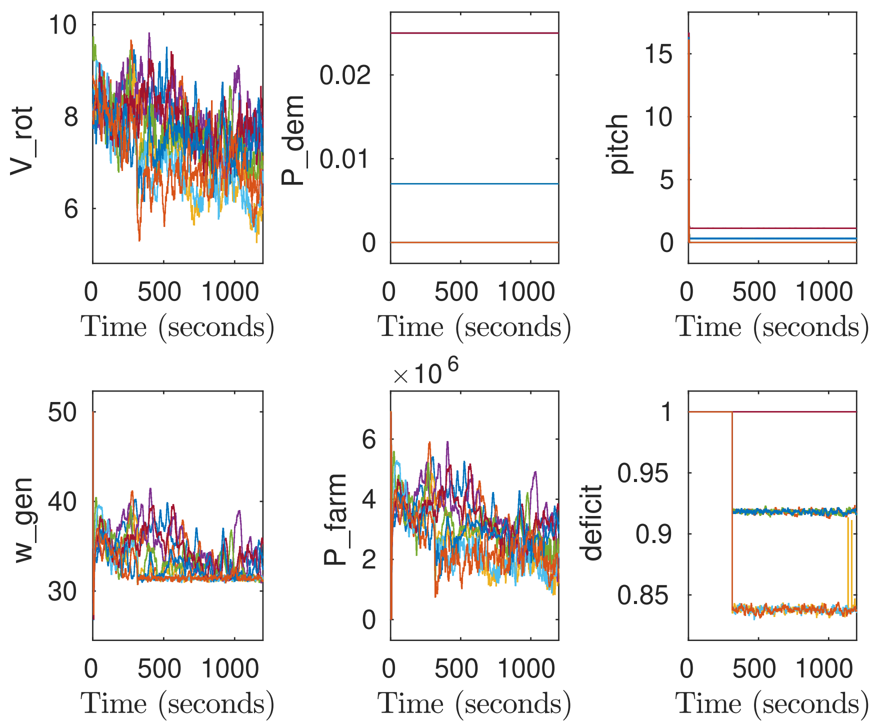

Figure 17. Example of time series from SimWindFarm simulation corresponding to the first row in table 11. Turbines has individual colors. Legends: V_rot: effective wind speed (m/s), P_dem: relative derating reference, w_gen: generator speed (rad/s), P_farm: wind turbine power (w), deficit: wake deficit at turbines.

The (full size) CLWindcon 3x3 farm has been simulated for the 4 directions and for both optimal and greedy control which makes 8 simulations which are shown in the first four blocks in table 11. The bottom block holds the average of the four direction results above. The statistic results are shown in table 11. In SimWindFarm a initial step generates the ambient wind field that would have been in the farm without turbines. The wakes are included during the time simulation of SimWindFarm in Simulink. In table 11 the first column “V_amb” is the average of the ambient wind field over both time and space. The remaining columns are also statistics over both time and turbines. For example “V_rot” is the time averages effective wind speed at a turbine averaged over the turbines. Similarly with “P_farm”. “M_shaft_std” and “M_tow_std” are the standard deviations for main shaft and tower torque which are used as a proxy for fatigue. The (scaled) damage equivalent load are found in “M_shaft_DEL” and “M_tow_DEL”.

Notice that for a particular direction and farm size the same wind field is used for both optimal and greedy control. In this way the small differences due to control are easier seen. An option for the experimental design would be to try to use the same wind field for all simulations so the effect of farm size would also be easier detectable but then dependent on only one wind field. This is however not possible with SimWindFarm where the ambient wind field is generated according to the geometry. Therefore there is one realization of the ambient wind field for each direction and farm size.

Operation	V_amb	V_rot	P_farm	M_shaft_std	M_tow_std	M_shaft_DEL	M_tow_DEL
	Wind direction 0 deg.						
Optimal	7.920	7.168	2.609e+6	6.689e+5	8.330e+6	1.113e+6	1.486e+7
Greedy		7.128	2.581e+6	6.832e+5	8.497e+6	1.136e+6	1.517e+7
Optimal/Greedy		1.006	1.011e+0	9.792e-1	9.803e-1	9.796e-1	9.794e-1
	Wind direction 30 deg.						
Optimal	8.063	7.642	3.172e+6	6.727e+5	9.730e+6	1.095e+6	1.730e+7
Greedy		7.631	3.165e+6	6.777e+5	9.819e+6	1.108e+6	1.745e+7
Optimal/Greedy		1.001	1.002e+0	9.926e-1	9.910e-1	9.882e-1	9.916e-1
	Wind direction 60 deg.						
Optimal	7.938	7.903	3.490e+6	6.196e+5	1.050e+7	1.057e+6	1.906e+7
Greedy		7.902	3.489e+6	6.202e+5	1.052e+7	1.059e+6	1.909e+7
Optimal/Greedy		1.000	1.000e+0	9.990e-1	9.985e-1	9.986e-1	9.986e-1
	Wind direction 90 deg.						
Optimal	8.095	7.463	2.977e+6	7.158e+5	9.303e+6	1.117e+6	1.581e+7
Greedy		7.381	2.939e+6	7.284e+5	9.693e+6	1.143e+6	1.639e+7
Optimal/Greedy		1.011	1.013e+0	9.827e-1	9.598e-1	9.777e-1	9.643e-1
	Average over wind direction.						
Optimal	8.004	7.544	3.062e+6	6.692e+5	9.465e+6	1.096e+6	1.676e+7
Greedy		7.511	3.044e+6	6.774e+5	9.631e+6	1.111e+6	1.703e+7
Optimal/Greedy		1.004	1.006e+0	9.880e-1	9.828e-1	9.858e-1	9.843e-1

Table 11. Results for full sized farm. Legends: V_amb: ambient wind speed, V_rot: effective wind speed, P_farm: wind turbine power, M_shaft_std: main shaft torque std, M_tow_std: tower torque std, M_shaft_DEL: main shaft torque DEL and M_tow_DEL: Tower torque DEL. See text for further details.

Table 11 clearly shows that the optimal control are always slightly better than the greedy. The two DEL’s are slightly lower and the power slightly higher. The bottom block shows a power fraction between optimal and greedy of 1.006. The corresponding figure in the Jensen analysis was

0.4392/0.4337 = 1.0127 which led to a possible size reduction of 6%. As the power increase due to control in table 11 is 0.6% against the Jensen 1.27% the size reduction will be reduced from the Jensen 6% to 3%. This also aligns with the Jensen analysis being on one row where the SimWindFarm results for the 3x3 CLWindcon farm has very small improvement for two out of four direction.

Eight more SimWindFarm simulations similar to the above ones are conducted. The difference is that the farm geometry is now reduced with a factor 0.97 in length scale and the wind field are four new realizations. The results for the squeezed farm are show in table 12 whits is organized exactly as table 11 for the full size farm. Also for the Squeezed farm the optimal control are producing more power and less fatigue compared to greedy control.

Operation	V_amb	V_rot	P_farm	M_shaft_std	M_tow_std	M_shaft_DEL	M_tow_DEL
	Wind direction 0 deg.						
Optimal	8.019	7.441	2.944e+6	6.307e+5	8.346e+6	1.043e+6	1.530e+7
Greedy		7.398	2.920e+6	6.408e+5	8.563e+6	1.070e+6	1.567e+7
Optimal/Greedy		1.006	1.008e+0	9.842e-1	9.746e-1	9.752e-1	9.766e-1
	Wind direction 30 deg.						
Optimal	7.974	7.574	3.085e+6	7.112e+5	9.948e+6	1.095e+6	1.629e+7
Greedy		7.562	3.075e+6	7.181e+5	1.001e+7	1.105e+6	1.640e+7
Optimal/Greedy		1.002	1.003e+0	9.905e-1	9.935e-1	9.904e-1	9.927e-1
	Wind direction 60 deg.						
Optimal	7.989	8.015	3.652e+6	6.846e+5	1.143e+7	1.084e+6	1.950e+7
Greedy		8.014	3.651e+6	6.853e+5	1.145e+7	1.086e+6	1.953e+7
Optimal/Greedy		1.000	1.000e+0	9.990e-1	9.984e-1	9.989e-1	9.984e-1
	Wind direction 90 deg.						
Optimal	8.091	7.219	2.644e+6	7.014e+5	8.591e+6	1.145e+6	1.465e+7
Greedy		7.129	2.593e+6	7.193e+5	8.893e+6	1.187e+6	1.510e+7
Optimal/Greedy		1.013	1.020e+0	9.751e-1	9.660e-1	9.642e-1	9.701e-1
	Average over wind direction.						
Optimal	8.018	7.562	3.081e+6	6.820e+5	9.580e+6	1.092e+6	1.643e+7
Greedy		7.526	3.060e+6	6.909e+5	9.730e+6	1.112e+6	1.668e+7
Optimal/Greedy		1.005	1.007e+0	9.871e-1	9.845e-1	9.818e-1	9.855e-1

Table 12. Results for squeezed farm. Legends: see table 11.

As some results can be difficult to see from the many numbers in table 11 and 12 figure 18 shows the farm power as a function of ambient wind speed and direction. All 16 simulations are in the 3D plot. The control and farm factor are indicated using colors and markers as shown in figure 19. In the 3D plot the differences do to control are not easy to distinguish as it disappears in other variation. Looking carefully at the 3D plot the wind direction is seen to give the largest variation. This becomes more clear in the 2D plot in figure 19. Here a number of observations can easily be done:

- The optimal control is always at least as good as the greedy.
- The wind direction given the wake pattern are the most important factor. 60 degrees gives more power than 30 degrees that gives more power than 0 and 90 degrees.

- The farm size factor effect seems to be hidden in other variation.

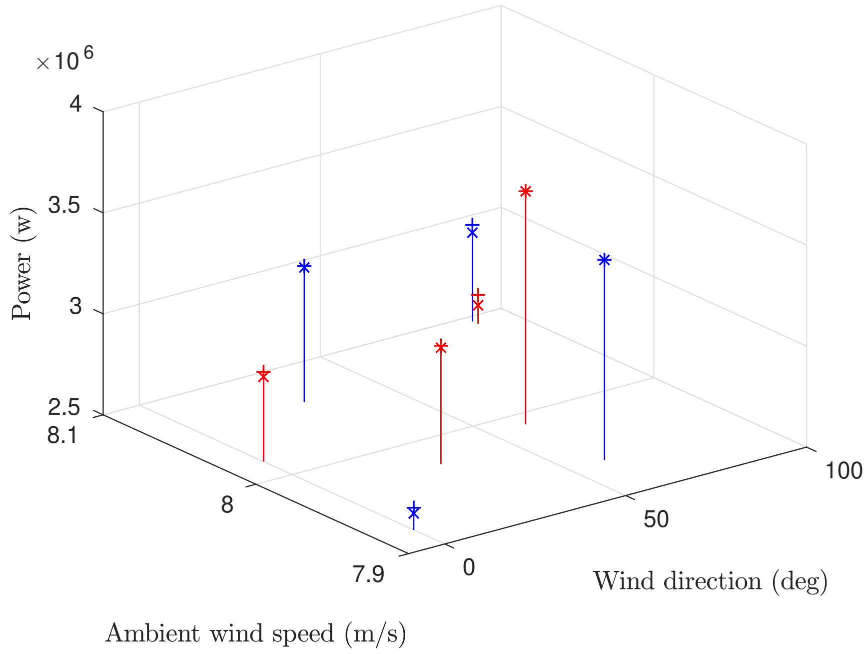

Figure 18. 3D graphical representation of the farm power from table 11 and 12 as a function of ambient wind speed and direction. Legends: see figure 19

To answer the two questions asked in section 3.2 the necessary results from table 11 and 12 are collected in the first block of table 13. The bottom block of table 13 clearly shows that when changing from the full sized greedy controlled farm to a squeezed farm optimal control outperforms greedy control as the relative power is higher and the relative fatigue lower. This gives a positive answer to the first question in section 3.2 which was also expected. The second question was about how much the full size greedy control farm can be squeezed before the optimal control can not make up for the squeezing effect on power. The row marked "Optimal-Sq/Greedy-FS" in table 13 shows that the 3% size reduction gives a relative farm power of 1.012. The complication is that the ambient wind speed factor is 1.002. If the power is assumed to follow the cubed power law this will give a power factor of $1.002^3 = 1.006$. As the power factor of 1.012 is higher than 1.006 and the fatigue DEL factors are lower than 1 it is concluded that the effect of 3% size reduction can be mitigated by the optimal control.

Operation-Farm	V_amb	V_rot	P_farm	M_shaft_std	M_tow_std	M_shaft_DEL	M_tow_DEL
Optimal-Sq	8.018	7.562	3.081e+6	6.820e+5	9.580e+6	1.092e+6	1.643e+7
Greedy-Sq	8.018	7.526	3.060e+6	6.909e+5	9.730e+6	1.112e+6	1.668e+7
Greedy-FS	8.004	7.511	3.044e+6	6.774e+5	9.631e+6	1.111e+6	1.703e+7
Optimal-Sq/Greedy-FS	1.002	1.007	1.012e+0	1.007e+0	9.947e-1	9.825e-1	9.652e-1
Greedy-Sq/Greedy-FS	1.002	1.002	1.005e+0	1.020e+0	1.010e+0	1.001e+0	9.794e-1

Table 13. Comparision of going from greedy control of full size farm to either greedy control of a squeezed farm or optimal control of a squeezed farm. Legends: see table 11.

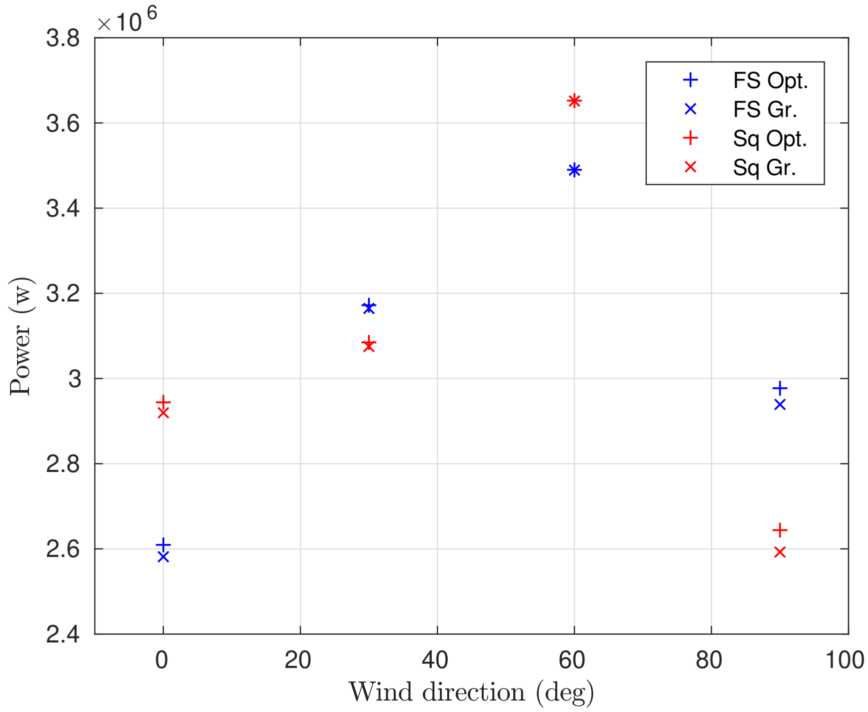

Figure 19. Plot of farm power from table 11 and 12 as a function ambient direction. Legends: FS: full size farm, Sq: squeezed farm, Opt.: Optimal control, Gr.: Greedy control. Notice that some of the values are on top of each other.

4 CONCLUSIONS

An optimization of NORCOWE wind farm has been carried out to find the optimum wind turbines position as well as optimum yaw setting with the annual energy production (AEP) as the objective function. The optimizations were carried out using WISDEM (Wind-Plant Integrated System Design and Engineering Model) and OpenMDAO (Multidisciplinary Analysis and Optimization) with SLSQP (Sequential Least SQuares Programming) as optimization algorithm. The used wake model is the parametric wind turbine wake model FLORIS (FLOw Redirection and Induction in Steady-state). FLORIS-SE - a plugin of WISDEM - and the assembly within OpenMDAO were adapted to run optimizations with the given wind measurement data of FINO3 and the DTU 10MW RWT.

The results showed that in the chosen scenario the position optimization with an increase of 34.0% in AEP is more effective than yaw optimization with 8.4%. Regarding optimization time, yaw optimization is faster with 35.7 hours than the position optimization with 47.3 hours. In the combined optimization case, the position-only optimized layout was in a next step optimized over yaw of turbines. Because of the large distances between the turbines in the optimized layout, the achieved improvement through a yaw optimization compared to the position-only optimization is only +0.04%.

A redesign of wind farm using induction control carried out to investigate the possibility of using induction control only to gain some of the performance loss of squeezing a otherwise uncontrolled wind farm. Analysis using static Jensen models for one row of turbines shows that 3 turbines in the wind direction can be squeezed 6% and the power gain by control will still balance with the power loss from squeezing. The Jensen analysis is also used to calculate optimal feed forward derating control settings using the “OpenDiscon” turbine controller from D2.1. For time domain simulations SimWindFarm is used. The farm considered is the 3x3 CL-Windcon wind farm from Deliverable D1.1 [3]. The experimental conditions are ambient wind speed 8 m/s and uniform direction distribution that are represented by four direction 0, 30, 60, 90. For the simulation test the 6% farm squeezing suggested by the one row Jensen analysis has been reduced to 3% as the average effect wake effect due to changing directions are at most 50%. The main simulation results are that the optimal feed forward control improves the power performance between 0.5 and 1%. This leads to a squeezing of the farm length scale by 3% with out loosing power performance and actually with improved fatigue performance for main shaft and tower.

REFERENCES

[1] C. Bak, F. Zahle, R. Bitsche, T. Kim, A. Yde, L. Henriksen, P. B. Andersen, A. Natarajan, and M. H. Hansen. "Design and performance of a 10 MW wind turbine." In: *Wind Energy* 124 (2013).

[2] P. Cheng. "Windenergienutzung 2 & Modul Windenergie 2." Script for the lecture. 2018.

[3] CL-Windcon project 2018 Deliverable D1.1. *Definition of reference wind farms and simulation scenarios*. http://www.clwindcon.eu.

[4] CL-Windcon project 2018 Deliverable D4.2. *Hardware and infrastructure conditions for energy capture and fatigue improvements*. http://www.clwindcon.eu.

[5] B. M. Doekemeijer, P. A. Fleming, and J.-W. van Wingerden. "A tutorial on the synthesis and validation of a closed-loop wind farm controller using a steady-state surrogate model." In: *American Control Conference Philadelphia July 10-12*. Version included in D2.3. IEEE/IFAC. IEEE, 2019.

[6] K. Dykes et al. *WISDEM 0.1.0 Documentation*. http://wisdem.github.io/WISDEM/. Accessed: 2019-04-10.

[7] K. Dykes, P. Graf, N. A. Scott George, R. King, Y. Guo, T. Parsons, R. Damiani, and P. Veers. *Introducing WISDEM Integrated System Modeling for Wind Turbines and Plants*. https://nwtc.nrel.gov/system/files/SE%20Webinar%202014-10-08.pdf. 2014.

[8] *FINO3 - research platform in the North Sea and the Baltic No. 3*. https://www.fino3.de/en/.

[9] *FLORISSE GitHub repository*. https://github.com/WISDEM/FLORISSE. Accessed: 2019-06-21.

[10] P. M. Gebraad, F. Teeuwisse, J.-W. van Wingerden, P. A. Fleming, S. D. Ruben, J. R. Marden, and L. Y. Pao. "A data-driven model for wind plant power optimization by yaw control." In: *2014 American Control Conference*. IEEE. 2014, pp. 3128–3134.

[11] J. Gray, K. Moore, and B. Naylor. "OpenMDAO: An open source framework for multidisciplinary analysis and optimization." In: *13th AIAA/ISSMO Multidisciplinary Analysis Optimization Conference*. 2010, p. 9101.

[12] R. Hoppe. "Optimization Theory." 2006.

[13] Á. Jiménez, A. Crespo, and E. Migoya. "Application of a LES technique to characterize the wake deflection of a wind turbine in yaw." In: *Wind energy* 13.6 (2010), pp. 559–572.

[14] S. Kiranyaz, T. Ince, and M. Gabbouj. *Multidimensional particle swarm optimization for machine learning and pattern recognition*. Springer, 2014.

[15] T. Knudsen, T. Bak, and M. Svenstrup. "Survey of wind farm control - power and fatigue optimization." In: *Wind Energy* 18.8 (May 13, 2014). Published online 9 May 2014 in Wiley Online Library (onlinelibrary.wiley.com), pp. 1333–1351.

[16] *NORCOWE reference wind farm*. https://rwf.computing.uni.no/about/. Accessed: 2019-05-21.

[17] NREL. *FLORIS. Version 1.0.0*. 2019. URL: https://github.com/NREL/floris.

[18] *OpenMDAO Documentation v0.13.* http://openmdao.org/releases/0.13.0/docs/index.html. Accessed: 2019-04-10.

[19] *OpenMDAO User Guide Version 0.13.0*. http://openmdao.org/releases/0.13.0/docs/index.html.

[20] M. Papageorgiou, M. Leibold, and M. Buss. *Optimierung*. Springer, 1991.

[21] F. R. "The Sequential Quadratic Programming Method." In: *Nonlinear Optimization. Lecture Notes in Mathematics*. Ed. by G. D. Pillo and F. Schoen. Vol. 1989. Berlin, Heidelberg: Springer, 2010.

[22] R. Shakoor, M. Y. Hassan, A. Raheem, and Y.-K. Wu. "Wake effect modeling: A review of wind farm layout optimization using JensenŒş s model." In: *Renewable and Sustainable Energy Reviews* 58 (2016), pp. 1048–1059.

[23] J. Thomas, E. Tingey, and A. Ning. "Comparison of two wake models for use in gradient-based wind farm layout optimization." In: *2015 IEEE Conference on Technologies for Sustainability (SusTech)*. IEEE. 2015, pp. 203–208.

[24] J. J. Thomas, P. M. Gebraad, and A. Ning. "Improving the FLORIS wind plant model for compatibility with gradient-based optimization." In: *Wind Engineering* 41.5 (2017), pp. 313–329.

[25] W. Tong, S. Chowdhury, J. Zhang, and A. Messac. "Impact of different wake models on the estimation of wind farm power generation." In: *12th AIAA Aviation Technology, Integration, and Operations (ATIO) Conference and 14th AIAA/ISSMO Multidisciplinary Analysis and Optimization Conference*. 2012, p. 5430.

[26] *Windenergiemarkt in Deutschland*. https://www.windbranche.de/windenergie-ausbau/deutschland. Accessed: 2019-04-10.

[27] *Wind_rose*. https://www.mathworks.com/matlabcentral/fileexchange/17748-wind_rose. Accessed: 2019-04-04.

[28] *WISDEM*. https://nwtc.nrel.gov/WISDEM. Accessed: 2019-04-10.

[29] S. Wright and J. Nocedal. "Numerical optimization." In: *Springer Science* 35.67-68 (1999), p. 7.